Supporting Information

DeGiuli et al. 10.1073/pnas.1415298111

Here we provide details of the variational argument discussed in the main text (section A), details of EMT (section B), evidence that including localized modes does not improve the variational argument (section C), information on the hard sphere numerical simulations (section D), information on the soft-sphere numerical simulations (section E), and evidence that the change in gap distribution at finite δz does not affect our results (section F).

A. Variational Argument

In the main text we present a variational argument to bound the density of vibrational states $D(\omega)$, using the floppy modes created when bonds are cut from systems near z_c. Here we present the details of this argument.

First, we recall the argument of refs. 1 and 2, where bonds are cut in blocks of size L. This requires cutting a fraction $q \sim 1/L$ of bonds. For a system at $\delta z = 0$, the density of induced floppy modes per particle is simply $(dN - (1-q)N_c)/(dN) = q \sim 1/L$. The floppy modes will have large displacements at the cut bonds. To create low-energy trial modes, we modulate the floppy modes by plane waves of wavelength $2L$, with nodes at the cut bonds. It can be computed that after this distortion, the modes have a frequency $\omega(q) \sim \omega_c/L \sim \omega_c q$ in the original, uncut system (1). A variational inequality (3) implies that the number of modes per particle with frequency smaller than ω, $\mathcal{N}(\omega)$, satisfies $\mathcal{N}(\sqrt{2}\omega) \geq q(\sqrt{2}\omega)/2$. In terms of scaling, this implies $\mathcal{N}(\omega) \gtrsim q(\omega)$. The results discussed in the main text follow.

Now we consider the modes created when the fraction q of weakest links are cut, inducing a density $q - \delta z/z_c$ of floppy modes. We make the key assumption that these floppy modes do not decay appreciably with distance from the broken bonds, but extend in the entire system, displacing particles by some characteristic amplitude. On the one hand, this assumption is supported by the proof that in an isostatic system the response to a local strain does not decay as a power law of distance (2), unlike what occurs in a normal (well-connected) elastic medium. On the other hand, this argument does not exclude the possibility that floppy modes have a very large amplitude just where the contacts were cut, and then a small background displacement not decaying with distance. As discussed in the main text, when we apply our results to hard spheres our assumption only holds for a fraction of the contacts at low force.

By definition, the displacements of floppy modes are strictly perpendicular to bonds, except at the broken bonds themselves. In particular, if we cut the bond β, $\delta R_\gamma^\parallel = 0$ for all $\gamma \neq \beta$. Our assumption that floppy modes are extended means that $\delta R_\beta^\parallel \sim \langle |\delta \vec{R}_i| \rangle \sim 1/\sqrt{N}$, where the average is made on all particles i and the last equation reflects normalization.

Let $\delta z \equiv z - z_c > 0$. The fraction q of weakest extended bonds has a characteristic stiffness k_0 with $\int_0^{k_0} \mathbb{P}(k)dk = q$, leading to $k_0 \sim k_c q^{1/(1+\alpha)}$. A density $q - \delta z/z_c$ of modes in the system is floppy. In the original system, these modes stretch or compress the fraction q of weak springs of characteristic stiffness k_0, and thus have a finite energy of order $E \propto \sum_\beta k_\beta \delta R_\beta^{\parallel 2} \sim qNk_0 1/N = qk_0$, leading to a characteristic frequency

$$\omega(q) \propto \sqrt{\frac{E}{m}} \sim \omega_c q^{\frac{2+\alpha}{2+2\alpha}}. \quad \text{[A1]}$$

The variational inequality implies $D(\omega) \gtrsim (q - \delta z/z_c)/\omega$. This argument can be applied with any $q \ll 1$ such that $q > \delta z/z_c$, implying that $\omega \gtrsim \omega_c (\delta z/z_c)^{(2+\alpha)/(2+2\alpha)}$. It is convenient to let $q = r\delta z$ with $r > 1/z_c$. Then

$$D(\omega) \gtrsim \frac{r - \frac{1}{z_c}}{\omega_c} \left(\frac{\omega}{\omega_c}\right)^{\frac{\alpha}{2+\alpha}} \quad \text{[A2]}$$

This leads to our central results discussed in the main text.

Assuming harmonic dynamics and equipartition, the covariance matrix of displacements, $\mathcal{C}_{ij} \equiv \langle \delta \vec{R}_i \delta \vec{R}_j \rangle$, is related to the matrix $\mathcal{M}_{ij}$ by $\mathcal{C}_{ij} = k_B T \mathcal{M}_{ij}^{-1}$. Taking the trace of this expression, we find the particles' mean-squared displacement

$$\frac{\langle \delta R^2 \rangle}{k_B T} = \frac{1}{N} \sum_i \mathcal{M}_{ii}^{-1} = \frac{1}{N} \sum_\omega \frac{1}{m\omega^2} = \int d\omega \frac{D(\omega)}{m\omega^2}. \quad \text{[A3]}$$

Using [A2] and $k_c/\omega_c^2 = m$, we obtain the bound

$$\frac{k_c \langle \delta R^2 \rangle}{k_B T} = \omega_c^2 \int \frac{D(\omega)}{\omega^2} d\omega > \omega_c^2 \int_{\omega > \omega^*} \frac{D(\omega)}{\omega^2} d\omega \gtrsim \left(\frac{\omega^*}{\omega_c}\right)^{\frac{-2}{2+\alpha}}. \quad \text{[A4]}$$

To estimate the shear modulus, we cut a fraction $q = 2\delta z/z_c$ of the weakest links, so that the system is now floppy with a density of floppy modes $\delta z/z_c$, and no elasticity. It was shown (4, 5) that under an applied shear of strain ε, the relative displacement of particles (of order of the nonaffine displacement) is of order $\epsilon/\sqrt{\delta z}$, as observed numerically (4, 6, 7). In the uncut system, this deformation has energy $\delta E \sim qk_0(q)(\epsilon/\sqrt{\delta z})^2$, leading to a shear modulus

$$\mu \sim k_0 \sim k_c \delta z^{\frac{1}{1+\alpha}}. \quad \text{[A5]}$$

B. Effective Medium Theory

Our EMT is an extension of ref. 8. The difference in the present work is to allow the bond stiffnesses and contact forces to follow nontrivial distributions $\mathbb{P}(k)$ and $\mathbb{P}(f)$. For the latter, we consider

$$\mathbb{P}(f) = C_f f^\theta e^{-\frac{f}{\bar{f}}}, \quad \text{[B1]}$$

($\theta = \theta_f$ in the main text) with $0 \leq \theta < 1$ and contact force law

$$f = k_1 |h|^x, \quad \text{[B2]}$$

where h is the gap at a contact ($h < 0$ for overlap). We are interested in the cases $-1 \leq x < 0$ and $x > 1$: The former ($x < 0$) corresponds to hard particles, and the latter ($x \geq 1$) corresponds to soft particles. We do not consider cusp-like potentials $0 < x < 1$. We assume particle diameter $\sigma = 1$ so that k_1 has units of stiffness. The contact stiffness is $k = -df/dh \propto |h|^{x-1}$. This implies

$$\mathbb{P}(k) = C_k k^\alpha e^{-\left(\frac{k}{\bar{k}}\right)^{\frac{x}{x-1}}}, \quad \text{[B3]}$$

with $\alpha = (1 + x\theta)/(x-1)$. We have $\alpha > 0$ when $x > 1$ and $\alpha < 0$ when $x < 0$. The contact strain e is defined by $e \equiv \langle f \rangle / \langle k \rangle$. We take units with $\bar{k} = 1$.

As in previous work (8), we model a random elastic network of coordination z by diluting a regular lattice of coordination z_0 down to z. The stiffness in contact α, k_α, and the force in the contact, f_α are random variables distributed according to

$$\mathbb{P}_{EMT}(k_\alpha) = (1-P)\delta(k_\alpha) + P\mathbb{P}(k_\alpha) \quad \textbf{[B4]}$$

$$\mathbb{P}_{EMT}(f_\alpha) = (1-P)\delta(f_\alpha) + P\mathbb{P}(f_\alpha), \quad \textbf{[B5]}$$

where $P = z/z_0$ to model the random dilution of the lattice.

In EMT, the elastic behavior of a random material, such as our randomly diluted lattice, is modeled by a regular lattice with effective frequency-dependent stiffnesses; as in ref. 8, we will have a longitudinal stiffness, $k^\parallel$, and a transverse stiffness, $-ek^\perp$. Writing $\overline{\cdot}$ for the disorder average, the EMT equations are, from ref. 8 (correcting several typos in that work),

$$0 = \overline{\frac{k^\parallel - k_\alpha}{1-(k^\parallel - k_\alpha)G^\parallel}} = \overline{\frac{ek^\perp - f_\alpha}{1+(ek^\perp - f_\alpha)G^\perp}}, \quad \textbf{[B6]}$$

where $G^\parallel$ and $G^\perp$ are related to the Green's function $\boldsymbol{G}(\omega) = (\mathcal{M} - m\omega^2)^{-1}$ by

$$G^\parallel = \boldsymbol{n}_\alpha \cdot \langle\alpha|\boldsymbol{G}|\alpha\rangle \cdot \boldsymbol{n}_\alpha \quad \textbf{[B7]}$$

$$G^\perp = \frac{1}{d-1}\left[\mathrm{tr}\left(\langle\alpha|\boldsymbol{G}|\alpha\rangle\right) - G^\parallel\right], \quad \textbf{[B8]}$$

with $\langle\alpha| \equiv \langle i| - \langle j|$. In the present case this leads to

$$0 = \frac{(1-P)k^\parallel}{1-k^\parallel G^\parallel} + \frac{PC_k}{G^\parallel}\left[-\frac{1}{C_k} + \frac{\beta}{G^\parallel}\int_0^\infty df \frac{f^\theta e^{-f}}{c+f^\beta}\right] \quad \textbf{[B9]}$$

$$0 = \frac{(1-P)ek^\perp}{1+ek^\perp G^\perp} + \frac{PC_f}{G^\perp}\left[\frac{1}{C_f} - \frac{\bar{f}^\theta}{G^\perp}\int_0^\infty df \frac{f^\theta e^{-f}}{c_2+f}\right], \quad \textbf{[B10]}$$

with $\beta = 1 - 1/x$, $c = (1-k^\parallel G^\parallel)/G^\parallel$, and $c_2 = (1+ek^\perp G^\perp)/(\bar{f}G^\perp)$. These equations need to be supplemented with an equation for $\boldsymbol{G}$. As in ref. 8, we consider a simplified continuum-like Green's function with a single elastic modulus, and whose isotropy has been restored. This is

$$\boldsymbol{G}(\boldsymbol{r},\omega) = \frac{z_0}{d}\hat{\boldsymbol{\delta}}\int_{BZ}\frac{d^dq}{(2\pi)^d}\frac{e^{i\boldsymbol{q}\cdot\boldsymbol{r}}}{(k^\parallel - \tilde{e}k^\perp)q^2 - m\omega^2}, \quad \textbf{[B11]}$$

where $BZ = \{\boldsymbol{q} : |\boldsymbol{q}| < \Lambda\}$ is an approximate first Brillouin zone, $\tilde{e} = (d-1)e$, and $\hat{\boldsymbol{\delta}}$ is the identity tensor. Isotropy of $\boldsymbol{G}$ implies an identity

$$G^\parallel = G^\perp = \frac{2d}{z_0}\frac{1}{k^\parallel - \tilde{e}k^\perp}\left(1 + \frac{m\omega^2}{d}\mathrm{tr}\left(\boldsymbol{G}(0,\omega)\right)\right). \quad \textbf{[B12]}$$

We solve Eqs. **B9–B12** in the limit $e \ll 1$ and $\delta z = z - z_c \ll 1$, for $\omega \ll 1$ (we now take $m = 1$). Based on previous results (8), we expect $|c| \ll 1$ and $|c_2| \gg 1$ (which can be checked a posteriori), which allows an expansion

$$\int_0^\infty df \frac{f^\theta e^{-f}}{c+f^\beta} = \begin{cases} -\dfrac{c^\alpha \pi}{\beta\sin(\pi\alpha)} + \ldots & \text{if} \quad -1 < \alpha < 0 \\ \Gamma_{\alpha\beta} + \ldots & \text{if} \quad \alpha > 0, \end{cases} \quad \textbf{[B13]}$$

with $\Gamma_t = \int_0^\infty x^{t-1}e^{-x}dx$. From this result it can deduced that for $\alpha > 0$, the previous results of ref. 8 are obtained, up to prefactors which depend on θ and x. Therefore, for soft particles with $\alpha \geq 0$, the scalings of ref. 8 are unchanged by stiffness heterogeneity, and henceforth we only consider the case $\alpha < 0$, corresponding to an abundance of weak springs, as discussed in the main text. The other integral is found similarly:

$$\int_0^\infty df \frac{f^\theta e^{-f}}{c_2+f} = \frac{\Gamma_{\theta+1}}{c_2} + \frac{\Gamma_{\theta+2}}{c_2^2} + \mathcal{O}\left(\frac{1}{c_2^3}\right). \quad \textbf{[B14]}$$

The leading order EMT equations are then

$$0 = k^\parallel G^\parallel - P + \frac{\left(1-k^\parallel G^\parallel\right)^{\alpha+1}P}{G^{\parallel\alpha+1}\Gamma_{\theta+1}}\frac{\pi}{\beta\sin(\pi|\alpha|)} \quad \textbf{[B15]}$$

$$0 = ek^\perp G^\perp - \frac{P\bar{f}G^\perp(\theta+1)}{1+ek^\perp G^\perp}. \quad \textbf{[B16]}$$

Assuming $\omega \ll \sqrt{k^\parallel/m}$, it can be checked that

$$\frac{1}{d}\mathrm{tr}\left[\boldsymbol{G}(0,\omega)\right] = \frac{A_1}{k^\parallel - \tilde{e}k^\perp} + \ldots, \quad \textbf{[B17]}$$

with

$$A_1 = \frac{z_0}{d}\frac{2\pi^{\frac{d}{2}}}{\Gamma_{\frac{d}{2}}(2\pi)^d}\begin{cases}\dfrac{\Lambda^{d-2}}{d-2} & \text{if} \quad d \geq 3 \\ \dfrac{1}{2}\log\dfrac{1}{\delta z} & \text{if} \quad d = 2.\end{cases} \quad \textbf{[B18]}$$

The above equations can be solved for $\delta z \ll 1$ following the procedure in ref. 8: We let

$$k^\parallel \sim \delta z^\xi, \quad ek^\perp \sim \delta z^\eta, \quad e = e_c e' \quad \textbf{[B19]}$$

$$e_c \sim \delta z^\chi, \quad \omega \sim \delta z^\zeta \quad \textbf{[B20]}$$

and balance terms in Eqs. **B15** and **B16**. Note that e and δz are independent parameters: In an elastic network they can be controlled independently. Here e_c is the critical contact strain at elastic instability (8). One finds

$$\xi = \frac{1}{\alpha+1}, \quad \textbf{[B21]}$$

$$\chi = \eta = 2\zeta = 1 + \xi = \frac{\alpha+2}{\alpha+1}, \quad \textbf{[B22]}$$

reproducing the scalings in the main text. To leading order, the transverse stiffness is

$$k^\perp = \frac{2d}{z_0}\frac{(\theta+1)\Gamma_{\theta+2-\frac{1}{x}}}{\Gamma_{\theta+2}} \quad \textbf{[B23]}$$

whereas the leading order equation for $k^\parallel$ is

$$0 = 2dA_1\omega^2 - k^\parallel\delta z + \tilde{e}k^\perp z_c + k^{\parallel\alpha+2}c_3, \quad \textbf{[B24]}$$

with $c_3 = \pi z_0(1-2d/z_0)^{\alpha+1}(z_0/(2d))^\alpha/(\Gamma_{\theta+1}\sin(\pi|\alpha|))$. This is a transcendental equation for $k^\parallel$ that does not have an analytic solution. However, we can determine some of its key properties.

We expect an onset frequency ω_0 where the density of states $D(\omega)$ grows from 0. This requires that at ω_0, $|dk^\parallel/d\omega| = \infty$, giving

$$\omega_0 = \omega^*\sqrt{1 - \frac{e}{e_c}}, \quad \textbf{[B25]}$$

with $\omega^* = \delta z^{\zeta}\sqrt{c_4/(z_c A_1)}$, $e_c = \delta z^{2\zeta} c_4/(2d(d-1)k^{\perp})$, and $c_4 = (c_3(\alpha+2))^{-1/(\alpha+1)}/\eta$. The onset frequency ω_0 vanishes at elastic instability $e = e_c$.

Below ω_0, $k^{\parallel} \approx k_*^{\parallel} \equiv k^{\parallel}(\omega_0) = (\delta z/(c_3(\alpha+2)))^{1/(\alpha+1)}$. For $\omega \gg \omega_0$, we find instead $k^{\parallel} \approx \omega^{2/(\alpha+2)}(-2dA_1/c_3)^{1/(\alpha+2)}$. Combining these gives the approximate solution

$$k^{\parallel} \approx k_*^{\parallel} + \omega^{\frac{2}{\alpha+2}}\left(-\frac{2dA_1}{c_3}\right)^{\frac{1}{\alpha+2}}. \qquad \textbf{[B26]}$$

The density of states is determined by

$$D(\omega) = \frac{z_0}{\pi\omega}\mathrm{Im}\left[\left(k^{\parallel} - \tilde{e}k^{\perp}\right)G^{\parallel}\right] \qquad \textbf{[B27]}$$

$$= \frac{2dA_1}{\pi}\omega\mathrm{Im}\left[\frac{1}{k^{\parallel} - \tilde{e}k^{\perp}}\right] + \ldots, \qquad \textbf{[B28]}$$

which readily gives

$$D(\omega) \sim \begin{cases} 0 & \text{if} \quad \omega < \omega_0 \\ \omega^{1+\frac{2}{\alpha+2}}\,\delta z^{-\frac{2}{\alpha+1}} & \text{if} \quad \omega_0 < \omega < \omega^* \\ \omega^{1-\frac{2}{\alpha+2}} & \text{if} \quad \omega > \omega^*. \end{cases} \qquad \textbf{[B29]}$$

Debye behavior is absent below ω_0, but would appear to next order in δz (8).

For a marginally stable material, $1 - e/e_c \ll 1$ so that $\omega_0 = 0$. Hard spheres correspond to $x = -1$ and $k_1 = k_B T \sim 1$ in our units. The predicted behavior in this case is shown in Fig. 2, for $d = 2$, corresponding to hard disks. Note that for hard disks, assuming $\theta \approx 0.41$, we have $\alpha = -0.30$, $1 + 2/(\alpha+2) = 2.17$, and $1 - 2/(\alpha+2) = -0.17$.

The shear modulus is $\mu = k^{\parallel}(\omega = 0)$. When $e = 0$, we find

$$\mu(e=0) = \left(\frac{\delta z}{c_3}\right)^{\frac{1}{\alpha+1}}, \qquad \textbf{[B30]}$$

whereas when $e = e_c$, $\mu(e = e_c) = k_*^{\parallel}$, so that μ is smaller by a factor of

$$\frac{\mu(e=0)}{\mu(e=e_c)} = (\alpha+2)^{\frac{1}{\alpha+1}} \qquad \textbf{[B31]}$$

at instability. Note that when $\alpha = 0$ we recover the factor 2 found in earlier theory (8, 9).

Finally, as in ref. 8 we can extract the asymptotic behavior of the Green's function for large r. To leading order, $\log(\boldsymbol{G}(r,\omega)) \sim -r/\ell_s(\omega) + i\omega r/\nu(\omega)$, where $\ell_s(\omega) = -\omega^{-1}|\Delta k|/\mathrm{Im}[\sqrt{\Delta k}]$ and $\nu(\omega) = |\Delta k|/\mathrm{Re}\left[\sqrt{\Delta k}\right]$ are, respectively, the scattering length and sound velocity at frequency ω. Here $\Delta k = k^{\parallel} - \tilde{e}k^{\perp}$. The former behaves as

$$\ell_s(\omega) \sim \begin{cases} \infty & \text{if} \quad \omega < \omega_0 \\ \omega^{-\frac{4+\alpha}{2+\alpha}}\,\delta z^{\frac{3}{2\alpha+2}} & \text{if} \quad \omega_0 < \omega < \omega^* \\ \omega^{-\frac{1+\alpha}{2+\alpha}} & \text{if} \quad \omega > \omega^*, \end{cases} \qquad \textbf{[B32]}$$

whereas the latter is instead

$$\nu(\omega) \sim \begin{cases} \delta z^{\frac{1}{2+2\alpha}} & \text{if} \quad \omega < \omega^* \\ \omega^{\frac{1}{2+\alpha}} & \text{if} \quad \omega > \omega^*. \end{cases} \qquad \textbf{[B33]}$$

We expect that a Rayleigh scattering regime would appear for $\omega < \omega_0$, at the next order in δz. From these results we note particularly that $\ell_s(\omega^*) \sim \delta z^{-1/2}$.

The above results give the leading order behavior when $\delta z \ll 1$. In $d = 2$, the next terms are smaller only by a factor $\sim 1/(\log 1/\delta z)$, leading to significant corrections. Therefore, the plot in Fig. 2 uses the full form of the Green's function, i.e.,

$$\frac{1}{d}\mathrm{tr}\left[\boldsymbol{G}(0,\omega)\right]\Big|_{d=2} = \frac{A_1}{\Delta k}\left[\log\left(\Delta k\Lambda^2 - \omega^2\right) - \log\left(-i0^+ - \omega^2\right)\right], \qquad \textbf{[B34]}$$

with $A_1 = z_0/(8\pi)$. In $d \geq 3$ the next terms are smaller by powers of δz and this problem does not arise.

C. Localized Modes

In the variational argument presented in the main text, we only opened those contacts that led to extended displacements. Here we show that also opening localized contacts, or some fraction of the two populations, do not improve this result.

We use the characterization of small forces described in ref. 10. Each contact $\alpha = \langle ij \rangle$ (between particles i and j) in an isostatic packing is opened, and the resulting displacement field is measured. Using the fact that the packing is isostatic, the contact force f_α can be written in terms of the resulting displacement field $\overrightarrow{\delta R}^{(\alpha)}$. In particular, each force can be written as

$$f_\alpha = f_c b_\alpha W_\alpha, \qquad \textbf{[C1]}$$

where f_c is a typical force, b_α characterizes the strength of far-field displacements relative to the displacements of i and j, and W_α characterizes the coupling strength between the displacement $\overrightarrow{\delta R}^{(\alpha)}$ and the confining stress (an isotropic pressure in the case considered). In particular, displacements scale as

$$\overrightarrow{\delta R}_i^{(\alpha)} \sim \overrightarrow{\delta R}_j^{(\alpha)} \sim C, \qquad \textbf{[C2]}$$

$$\overrightarrow{\delta R}_k^{(\alpha)} \sim bC, \quad k \neq i,j, \qquad \textbf{[C3]}$$

where $1/C^2 \sim 2 + b^2 N$ is a normalization constant.

A contact force can be small in two ways: Either the far-field displacement field has a small amplitude, $b_\alpha \ll 1$, corresponding to localized modes, or the displacement $\overrightarrow{\delta R}^{(\alpha)}$ is weakly coupled to the confining stress, $W_\alpha \ll 1$, corresponding to extended modes. For small values of b and W, it was found that

$$\mathbb{P}(b) \sim b^{\theta_\ell}, \mathbb{P}(W) \sim W^{\theta_e}, \qquad \textbf{[C4]}$$

and furthermore that b and W are approximately independent. We assume that $\theta_e > \theta_\ell$, as confirmed by numerics, and as implied by marginal stability relations discussed in the main text.

We want to allow, in the variational argument, the possibility of cutting weak links with a certain mix of localized and extended properties. A convenient way to do so is to cut links along the curve

$$b = W^{\eta} \qquad \textbf{[C5]}$$

in (b, W) space, with $0 < \eta < \infty$, so that $f \sim b^{1+1/\eta}$. When $\eta \to 0$, we cut links independently of b, corresponding exclusively to extended contacts. When $\eta \to \infty$, we cut links independently of W, corresponding exclusively to localized contacts.

Suppose we cut a fraction q of contacts from an isostatic packing. Then the induced $\sim qN$ floppy modes will have displacements scaling as in **[C2]**, but where i and j correspond to any of the particles adjacent to the cut contacts. Modifying accordingly the

normalization constant C, the energy of a typical mode in the original uncut system will be

$$E \sim \frac{qNk_0}{qN + b^2N} = \frac{qk_0}{q + b^2}, \quad \text{[C6]}$$

where the stiffness k_0 is determined by $q = \int_0^{k_0} \mathbb{P}(k)dk$. This corresponds to a force f_0 with $q = \int_0^{f_0} \mathbb{P}(f)df$. It follows after some algebra that $q \sim f_0^{1+(\eta\theta_\ell+\theta_e)/(1+\eta)}$ and $b^2 \sim q^{2\eta/(1+\eta+\eta\theta_\ell+\theta_e)}$. Fixing $q \ll 1$, the best bound is obtained by minimizing the energy $E(q)$ because this corresponds to the smallest frequency for a given amount of cut contacts, and therefore the largest $D(\omega(q)) \gtrsim q/\omega(q)$. There are two cases.

Case i: Predominantly Localized Contacts $q \gg b^2$. The condition $q \gg b^2$ requires $\eta > \eta_0$ with $\eta_0 = (1+\theta_e)/(1-\theta_\ell)$. In this case, $E \sim k_0 \sim f_0^2 \sim q^{g_1(\eta)}$ with $g_1(\eta) = 2(1+\eta)/(\eta+\eta\theta_\ell+1+\theta_e)$. It can be checked that $g_1'(\eta) > 0$ for all η, so that the energy is minimized at the largest value of η, i.e., $\eta \to \infty$. In this case,

$$E_{\eta\to\infty} \sim q^{\frac{2}{1+\theta_\ell}}. \quad \text{[C7]}$$

Case ii: Predominantly Extended Contacts $q \ll b^2$. The condition $q \ll b^2$ requires $\eta < \eta_0$. In this case, $E \sim qk_0/b^2 \sim q^{g_2(\eta)}$, with

$$g_2(\eta) = 1 + \frac{2}{1+\eta+\eta\theta_\ell+\theta_e}. \quad \text{[C8]}$$

It can be checked that $g_2'(\eta) < 0$ for all η, so that the energy is minimized at the smallest value of η, i.e., $\eta \to 0$. In this case,

$$E_{\eta\to 0} \sim q^{1+\frac{2}{1+\theta_e}}. \quad \text{[C9]}$$

Now we note that $1 + 2/(1+\theta_e) > 1 + 2/(1+1) = 2$ and $2/(1+\theta_\ell) < 2$. This implies that $E_{\eta\to 0} \ll E_{\eta\to\infty}$, and therefore the smallest energy is attained when choosing only the extended contacts.

D. Hard-sphere Numerical Simulations

We simulate hard disks using an event-driven molecular dynamics code (11) in which particles are in free flight until they collide elastically. The system is 50:50 bidisperse, with a size ratio of 1.4. We take units with small diameter $\sigma_1 = 1$, mass $m = 1$ (the same for both species), and $k_BT = 1$, so that time is measured in units of $\sqrt{m\sigma_1/(k_BT)}$. To generate very large packings, we start with random configurations at very low density and use the Lubachevsky–Stillinger algorithm, in which particles are inflated (12). The particle inflation rate Γ varies with pressure p as $\Gamma = 10^{-3}$ up to $p = 10^2$ and $\Gamma = 10^{-5}$ up to $p = 10^{12}$. At $p = 10^{12}$ the packing fraction is distributed around $\phi_c \approx 0.83$. This protocol generates isostatic packings at ϕ_c, as was explicitly checked in all of the packings used. To obtain configurations at $\phi < \phi_c$, particles are then deflated by a relative amount ε, and assigned random velocities. Note that $(1/2)Nzk_BT = p(V - V_c) \approx p(\phi_c - \phi)N3\pi/(2\phi_c^2)$ so that $p(\phi_c - \phi) \approx 0.29k_BT$.

To measure the vibrational spectrum of hard disks, it is necessary to define a contact force network within an interval of time τ (13, 14). Two particles are said to be in contact if they collide with each other during τ. In this same interval, we define h_{ij} as the average gap between two particles, and the contact force f_{ij} as the average momentum they exchange per unit of time. We can then define an effective potential $V_{eff} = -k_BT \log h_{ij}$ (13, 14), which allows a computation of the dynamical matrix $\mathcal{M}$. In this work we choose $\tau = 1{,}000N$ collisions and $N = 4{,}096$ particles. For larger τ, the vibrational spectrum does not change in the frequency range shown.

E. Soft-Sphere Numerical Simulations

We prepare 3D isostatic packings of bidisperse soft spheres, of which half are large and half are small, with the ratio of their respective radii set to 1.4. With ρ_i denoting the radius of the i^{th} particle, and r_{ij} denoting the pairwise distance between the centers of particles i and j, the pairwise potential reads $\phi(r_{ij}) = (k/2)(r_{ij} - (\rho_i + \rho_j))^2$, where k is the stiffness. We generate isostatic packings by performing a fast quench of a random configuration using the fast inertial relaxation engine (FIRE) algorithm (15) and applying compressive or expansive strains followed by additional quenches to obtain the target coordination of $z_c = 6$. We choose the stopping condition of the quenches to be $\|\vec{F}^{\max}\|/\langle f\rangle < 10^{-8}$, where $\|\vec{F}^{\max}\|$ is the magnitude of the maximum (over all particles in a packing) of the net force and $\langle f\rangle$ is the mean contact force. We note that for our largest systems of $N = 8{,}000$ particles, the isostatic point occurs at dimensionless pressures of the order 10^{-9} or smaller; equilibrating packings mechanically at such pressures requires quad floating point precision numerics.

For the sake of comparison, we have also prepared an ensemble of monodisperse isostatic packings of $N = 4{,}000$, using the same procedure described above. The associated distribution of contact forces $P(f)$ is presented in Fig. S1. We find $P(f) \sim f^{\theta_f}$ with $\theta_f \approx 0.22$, which is slightly larger than what we observe in the bidisperse isostatic packings, suggesting that θ_f might not be universal.

To obtain accurate statistics on force distributions, for the binary packings we used 1,000, 4,000, and 10,000 configurations for system sizes $N = 8{,}000$, $N = 1{,}000$, and $N = 124$, respectively. The distribution for the monodisperse packings are measured in 1,000 configurations of packings of $N = 4{,}000$ particles.

F. Effect of Change of Stiffness Distribution with ϕ

In the main text and in the EMT described above, we have assumed that the shape of the distribution of stiffnesses, $\mathbb{P}(k)$, is independent of δz and e. For hard spheres, we have $f = k_BT/h$ and $k = k_BT/h^2$, where h is the average gap between particles, given that they share a contact (in the sense of ref. 14). The main effect of changing ϕ is to rescale the characteristic stiffness k_0, which is included in our approach. However, as discussed in ref. 16, one expects the rescaled distribution of gaps (and therefore of stiffnesses) to evolve as ϕ departs from ϕ_c at weak forces. Here we argue that this evolution, and the presence of additional contacts at large distance and small force, does not alter our prediction on κ. For simplicity we shall consider that all particles at distance $h \lesssim 1$ share a contact (a scenario presumably much worse than what occurs in packings where contacts are plausibly not made as soon as $h \gg h_\dagger$ defined below). We let $k_BT = 1$.

The hard-sphere gap distribution $g(h)$ has two scaling regimes (denoted Ib and IIIb in ref. 16) and an intermediate matching regime (denoted IIb in ref. 16). In the first scaling regime, corresponding to gaps that become contacts in the limit $p \to \infty$, we have

$$g(h) \sim p(hp)^{-2-\theta_f} \quad \text{if} \quad h \sim p^{-1}. \quad \text{[F1]}$$

In the second scaling regime, corresponding to gaps that are small but not zero, as $p \to \infty$, we have

$$g(h) \sim h^{-\gamma} \quad \text{if} \quad h \sim 1. \quad \text{[F2]}$$

In ref. 16, these forms are shown to match smoothly in an intermediate regime $h \sim p^{-\mu}$ with $\mu = (1+\theta_f)/(2+\theta_f-\gamma)$. Here it will be sufficient to eliminate this intermediate regime by joining the two primary distributions at an intermediate gap size $h_\dagger \sim p^{-\mu}$. We also truncate $g(h)$ at microscopic and macroscopic gap sizes $\delta \ll p^{-1}$ and $h_L \sim 1$. We therefore consider

$$g(h) \sim \begin{cases} p(hp)^{-2-\theta_f} & \text{if} \quad \delta < h < h_\dagger \\ C_2 h^{-\gamma} & \text{if} \quad h_\dagger < h < h_L. \end{cases} \qquad \textbf{[F3]}$$

This implies

$$\mathbb{P}(k) = \frac{C_1}{k^{\frac{3}{2}}} \begin{cases} p\left(\frac{p}{\sqrt{k}}\right)^{-2-\theta_f} & \text{if} \quad k_\dagger < k < 1/\delta^2 \\ C_2 k^{\frac{\gamma}{2}} & \text{if} \quad k_L < k < k_\dagger, \end{cases} \qquad \textbf{[F4]}$$

where $k_L = 1/h_L^2$ and $k_\dagger = 1/h_\dagger^2$. The constants C_1 and C_2 in these expressions are set by requiring that $\mathbb{P}(k)$ is normalized, and the distribution is continuous at $h_\dagger$. This implies $C_2 = p^{-1-\theta_f} k_\dagger^{(2+\theta_f-\alpha)/2}$.

As discussed in the main text, we consider only the subset of extended contacts, in effect replacing θ_f with θ_e in this expression. Then because $-3/2+1+\theta_e/2=\alpha$ and the cutoff $1/\delta^2$ plays the same role as an exponential cutoff (as in Eq. **B3**), this distribution differs from what is considered in the main text by the ultraweak force regime $k < k_\dagger$. To show that the presence of this regime does not affect our results, we estimate its relative contribution to the energy in a typical mode, R, as

$$R = \frac{\int_{k_L}^{k_\dagger} dk\, k\, \mathbb{P}(k)}{\int_{k_\dagger}^{\frac{1}{\delta^2}} dk\, k\, \mathbb{P}(k)} \qquad \textbf{[F5]}$$

$$\sim p^{1+2\theta_e} \delta^{4+2\alpha}. \qquad \textbf{[F6]}$$

We can let $\delta \sim p^{-\nu}$ with $\nu \geq 1$, which implies $R \lesssim p^{\theta_e - 2}$. This goes to zero as $p \to \infty$, so to leading order the ultraweak springs contain only an infinitesimal fraction of energy, and will not affect our results.

We note that our prediction for $\delta z(p)$ discussed in the main text is satisfied in the numerics of ref. 16, if the contact network is assumed to consist of those particles whose gap is smaller than $h \sim h_\dagger$. Because our estimate of R assumes contacts are made for $h \lesssim 1$, we expect that R is in fact an upper bound on the contribution of the ultraweak forces.

1. Wyart M, Nagel S, Witten T (2005) Geometric origin of excess low-frequency vibrational modes in weakly connected amorphous solids. *EPL* 72(3):486–492.
2. Wyart M (2005) On the rigidity of amorphous solids. *Ann Phys* 30(3):1–113.
3. Horn A (1954) Doubly stochastic matrices and the diagonal of a rotation matrix. *Am J Math* 76(3):620–630.
4. Wyart M, Liang H, Kabla A, Mahadevan L (2008) Elasticity of floppy and stiff random networks. *Phys Rev Lett* 101(21):215501–215504.
5. Lerner E, Düring G, Wyart M (2012) Toward a microscopic description of flow near the jamming threshold. *EPL* 99(5):58003–58008.
6. Ellenbroek WG, Zeravcic Z, van Saarloos W, van Hecke M (2009) Non-affine response: Jammed packings vs. spring networks. *EPL* 87:34004–34009.
7. Ellenbroek WG, Somfai E, van Hecke M, van Saarloos W (2006) Critical scaling in linear response of frictionless granular packings near jamming. *Phys Rev Lett* 97(25):258001–258004.
8. DeGiuli E, Laversanne-Finot A, Düring G, Lerner E, Wyart M (2014) Effects of coordination and pressure on sound attenuation, boson peak and elasticity in amorphous solids. *Soft Matter* 10(30):5628–5644.
9. Yoshino H (2012) Replica theory of the rigidity of structural glasses. *J Chem Phys* 136(21):214108–214143.
10. Lerner E, Düring G, Wyart M (2013) Simulations of driven overdamped frictionless hard spheres. *Comput Phys Commun* 184:628–637.
11. Allen MP, Tildesley DJ (1989) *Computer Simulation of Liquids* (Oxford University Press, Oxford).
12. Donev A, Torquato S, Stillinger FH (2005) Pair correlation function characteristics of nearly jammed disordered and ordered hard-sphere packings. *Phys Rev E Stat Nonlin Soft Matter Phys* 71(1 Pt 1):011105.
13. Brito C, Wyart M (2006) On the rigidity of a hard-sphere glass near random close packing. *EPL* 76(1):149–156.
14. Brito C, Wyart M (2009) Geometric interpretation of previtrification in hard sphere liquids. *J Chem Phys* 131(2):024504.
15. Bitzek E, Koskinen P, Gähler F, Moseler M, Gumbsch P (2006) Structural relaxation made simple. *Phys Rev Lett* 97(17):170201.
16. Charbonneau P, Corwin EI, Parisi G, Zamponi F (2012) Universal microstructure and mechanical stability of jammed packings. *Phys Rev Lett* 109(20):205501.

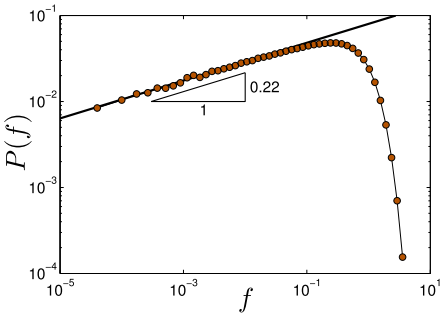

Fig. S1. Distribution of rescaled contact forces $P(f)$ measured in isostatic $N = 4,000$ packings of monodisperse harmonic spheres in three dimensions.